Results in Physics 53 (2023) 106968

Contents lists available at ScienceDirect

Results in Physics

journal homepage: www.elsevier.com/locate/rinp

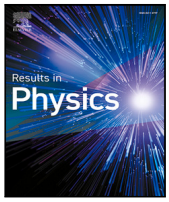

Optimal strategies for control of cholera in the presence of hyper-infective individuals

Baba Seidu [a], Eric N. Wiah [b], Joshua Kiddy K. Asamoah [c,d,*]

[a] Department of Mathematics, Faculty of Mathematical Sciences, C.K. Tedam University of Technology and Applied Sciences, Navrongo, Ghana, 0215-5321, UK
[b] Department of Mathematical Sciences, University of Mines and Technology, Takwa, Ghana
[c] Department of Mathematics, Kwame Nkrumah University of Science and Technology, Kumasi, Ghana
[d] Department of Mathematics, Saveetha School of Engineering SIMATS, Chennai, India

ARTICLE INFO

Keywords:
Cholera model
Stability
Sensitivity analysis
Optimal control theory
Basic reproduction number

ABSTRACT

Cholera is a potentially life-threatening bacterial infection caused by the bacterium *Vibrio cholerae*, with the primary site of infection being the small intestine. The disease typically spreads through contaminated water and food and becomes more pronounced in areas with poor sanitation and inadequate access to clean drinking water. Cholera infection can lead to severe diarrhoea, dehydration, and death if left untreated. Individuals with low personal hygiene have higher chances of spreading and/or contracting the disease. This study aims to propound a non-linear deterministic model to study the dynamics of cholera in the presence of two groups of individuals based on their level of personal hygiene. We categorize these individuals into low-risk and high-risk to describe individuals with good personal hygiene and those with very low personal hygiene, respectively. The model is shown to have two mutually exclusive fixed points, namely, the cholera-free and the cholera-persistent equilibria, indicating the presence of forward bifurcation. It is shown that restriction of the basic reproduction number below unity guarantees local asymptotic stability of the cholera-free fixed point. The immigration rate, rate of disinfection, bacteria ingestion rate, and bacterial shedding rate are parameters with a higher impact on cholera spread. Optimal control analysis is also used to determine the most cost-effective combination of infection control, adherence to sanitation protocols, treatment control, and bacterial-shedding controls needed to control the spread of cholera.

Introduction

Cholera, an acute bacterial infection caused by *Vibrio cholerae*, typically enters the human body when contaminated food or water is consumed. The transmission of cholera is attributed to person-to-person contact because the contamination of food and water frequently originates from faecal matter containing the bacteria. Within a short period (usually between 12 h to five days) after ingestion, the bacterium releases enterotoxins that can cause severe diarrhoea, leading to dehydration, vomiting, leg cramps, and even shock. Even though most people who ingest the bacterium do not fall sick, cholera can lead to death if proper, timely treatment is not given.

Cholera is perhaps among the topmost diseases that have been with man for centuries and persists even after several interventions to curb its spread. Despite significant progress in battling cholera in certain regions, the disease continues in most developing countries, where the availability of clean drinking water and proper sanitation facilities remains a significant challenge.

Roughly 1.3 billion individuals are susceptible to contracting cholera, resulting in approximately 1.3 million to 4 million cholera cases and 21,000 to 143,000 deaths caused by cholera each year [1]. Africa and Southern Asia continue to bear the brunt of the cholera infection as about 99% of all cases are from these regions [2]. The need to continue to seek a better understanding of the transmission dynamics of cholera cannot, therefore, be overemphasized.

Mathematical modelling has helped to increase the understanding of spreading and controlling infectious diseases, including cholera. From the work of Capasso and Paveri-Fontana [3], several models have been developed to account for different factors affecting the spread of cholera and its control. To study the role of the aquatic *V. cholerae*-reservoir, Codeco [4] extended the model of Capasso and Paveri-Fontana [3] by including a compartment for the environmental concentration of the pathogen. Rachael and colleagues [5] proposed an optimal control problem to provide a framework for designing cost-effective strategies for controlling Cholera. Using data from the various

* Corresponding author at: Department of Mathematics, Kwame Nkrumah University of Science and Technology, Kumasi, Ghana.
E-mail address: jkkasamoah@knust.edu.gh (J.K.K. Asamoah).

https://doi.org/10.1016/j.rinp.2023.106968
Received 2 July 2023; Received in revised form 26 August 2023; Accepted 8 September 2023
Available online 12 September 2023

provinces of Haiti to fit proposed mathematical models of Cholera to provide for predictions of morbidity and mortality and to study the impact of proposed interventions, Andrews and Basu [6] observed that reduced consumption of contaminated water, vaccination and extended administration of antibiotics to infected persons might help avert thousands of Cholera-related death in Haiti. Zhou and Cui [7] extended previous models to study the effect of vaccination on Cholera spread and observed that ensuring that the basic reproduction number does not exceed unity guarantees global stability of the cholera-free fixed point. Wang and Liao [8] used a generalized incidence function and generalized pathogen concentration to provide a unified compartmental model of Cholera and observed the presence of forward transcritical bifurcation, under some biologically reasonable conditions with the basic reproduction number being 1. Other important models proposed to study Cholera can be found in [9–13].

We note that most of the developed models have lumped susceptible individuals into one group. However, the chances of a susceptible person contracting cholera depends not only on the Infectives but also on the action or inaction of the susceptible person. Individuals who observe proper hygiene (by properly cooking foods, washing vegetables and fruits before eating, washing hands with soap under running water and regularly sanitizing of hands, among others) are less likely to get infected than those who do not observe these safety measures. Similarly, infected persons who observe proper safety measures are less likely to transmit the bacterium than those infectives who do not. In this study, we denote the individuals with poor or improper hygiene as high-risk because their characteristic predisposes them to spreading and/or contracting cholera. Also, those with proper hygiene are denoted as low-risk individuals because their characteristic helps in reducing their chances of spreading and/or contracting the disease. Susceptible and infective high-risk individuals are said to be hyper-susceptible and hyper-infective, respectively. The main goal of this study is to mathematically elucidate the role of hyper-susceptible and hyper-infective individuals in the spread of cholera. The research aims to study the impact of attitude towards safety measures in preventing the spread of cholera by segregating the susceptible and infective populations into two classes, each of those who observe the safety/preventive measures and those who do not. The methodology of incorporating different compartments to study the impact of different levels of adherence to safety protocols has been implemented in other previous studies [5,14,15].

We organized the rest of the paper as follows: The model under consideration is developed in the next section. Furthermore, the basic qualitative properties are discussed. Subsequently, an optimal control problem is constructed by introducing time-dependent controls into the basic model and seeking to minimize the hyper-susceptible population, infectives and the cost of implementing the controls. Numerical simulation is carried out to illustrate the analytical results obtained and determine (through the optimal control problem) the most cost-effective ways of controlling the spread of cholera. Lastly, we present the conclusion.

Model design

Attitude towards safety protocols in preventing transmission of Cholera plays a major role in the spread of the disease. Individuals with the right attitude towards hygiene can help reduce the transmission of Cholera. That is, Infected persons who take the needed steps to avoid transferring the bacterium and Susceptible persons who take steps to avoid contacting bacterial sources will help to reduce the spread of the disease. High-risk individuals can become low-risk if they drink safe water (bottled or boiled), maintain good hygiene (frequent handwashing with soap), thoroughly cook foods before eating, avoid contaminated sources, educate others about prevention, seek medical help for symptoms, and consider vaccination in high-risk areas. Therefore, it is important to study the impact of different levels of commitment towards the observation of the right attitude safety hygiene measures in combatting cholera. This study considers the outbreak of Cholera in a variable-sized population consisting of two groups of susceptibles and two groups of Infectives. The two groups of Susceptibles and Infectives are introduced to account for different levels of susceptibility and infectivity of Susceptibles and Infectives, respectively, resulting from the right attitude towards hygiene protocols. The different levels of susceptibility of people are introduced to track the impact of individuals who do not observe the appropriate levels of safety measures in protecting themselves from infection. Susceptible individuals who do not observe the necessary levels of sanitation protocols such as proper cooking of vegetables, drinking of clean water and washing of hands with soap under running water, thereby increasing their chances of getting exposed/infected with Cholera are referred to as high-risk susceptible individuals in this paper. Unlike the high-risk susceptible, those who observe proper hygiene are called low-risk persons because of their reduced chances of getting infected due to their behaviour. Also, the different levels of infectives are intended to track the impact of individuals who fail to comply with strategies to reduce the shedding of the bacterium into the environment. These Infectives who fail to observe the needed sanitation protocols such as washing hands with soap under running water, avoidance of open defecation and proper waste disposal, thereby increasing their chances of spreading cholera, are described in this work as high-risk Infectives or hyper-infective individuals. The counterparts of the high-risk infectives are referred to as low-risk infectives. To this end, the total human population at time t is divided into five mutually exclusive compartments of low-risk susceptibles $S_L(t)$, high-risk susceptibles, $S_H(t)$, low risk-infectives, $I_L(t)$, high-risk infectives, $I_H(t)$ and the recovered population, R, so that the total human population is given by $N(t) = S_L(t)+S_H(t)+I_L(t)+I_H(t)+R(t)$. The bacterial concentration in the environment at time t is $B(t)$. The human population is increased through a constant recruitment rate of Λ persons per unit of time, with a proportion f being high-risk and the remainder being low-risk. All recruits are assumed to be uninfected. Through health campaigns, high-risk individuals begin to practisce proper safety precautions such as proper washing of hands with soap under running water, cooking of vegetables and meat and avoiding open defecation and hence join the low-risk groups at a rate of α persons per unit time. The effect of media campaigns in reducing the number of infectives has been observed in previous studies [9, and others]. Susceptibles are assumed to get infected through contact with infected persons or consumption of Vibrio-contaminated food. The force of infection from infected persons is given by $\lambda_1 = \frac{\beta_h(t)(I_L+\eta_1 I_H)}{N}$ and the force of infection from consumption of Vibrio-contaminated food is given by $\lambda_2 = \frac{\beta_b B}{K+B}$. The parameters β_h and β_b measure the rate at which susceptibles ingest the bacterium from humans and the environment, respectively, while the parameters K and $\eta_1 > 1$ respectively are the half-saturation constant of the bacterium in contaminated water and food; and a modification parameter accounting for hyper-infectivity of high-risk Infectives. Infected persons are assumed to shed the bacteria into the environment at rate ξ through improper disposal of faecal matter. The parameter $\tau > 1$ accounts for increased bacterial shedding by hyper-infectious persons due to their non-compliance with proper hygiene protocols. Infected persons are assumed to recover from Cholera through treatment at ρ per unit time to join the recovered class who lose immunity at the rate of θ per unit time to join only the low-risk. Recovered individuals who lose immunity are assumed to join the low-risk persons because it is expected that they would have become more aware or hygiene-conscious due to the infection or exposure to hygiene advocacy during treatment. Natural and disease-induced death rates in humans are taken to be μ and μ_d respectively, while the bacterial-death rate (or rate of disinfection) is taken to be d. With these assumptions, the following coupled differential equations

Table 1
Descriptions and baseline values of model parameters.

Par.	Description	Baseline value	Ref
Λ	Recruitment rate into the human population	20/day	Assumed
f	Fraction of recruits who are high-risk	0.5	Assumed
α	Positive attitudinal change rate towards sanitation	0.25	Assumed
θ	Waning rate of recovery-conferred immunity	9.11×10^{-4}	Estimated from [16]
μ	Natural death rate among Humans	5.48×10^{-5}/day	[17]
μ_d	Cholera-induced death rate among Humans	0.015/day	[18]
$\eta_1(\eta_2)$	Hyper-infectivity(Susceptibility) parameter for I_H (S_H)	1.5(1.5)	Assumed
τ	Coefficient of bacterial shedding by Hyper-Infectives	2	Assumed
ξ	Bacterial Shedding rate by infectious Persons.	100 Cells/L-per day	[4]
ρ	Rate of recovery from cholera infection	0.004/day	[18]
β_b	Bacteria ingestion rate from environment	0.2143/day	[18]
β_h	Bacteria ingestion rate from humans	4×10^{-5}/day	Assumed
K	Concentration of Vibrio cholerae	10^9 Cells/L	[18]
d	Rate of removal of *V. cholerae*	0.33/day	[4]

give the cholera model of interest.

$$\left.\begin{aligned}
\frac{dS_L}{dt} &= (1-f)\,\Lambda + \alpha\, S_H + \theta\, R - \left(\lambda_1+\lambda_2+\mu\right) S_L,\\
\frac{dS_H}{dt} &= f\,\Lambda - \left(\eta_2\lambda_1+\eta_2\lambda_2+\alpha+\mu\right) S_H,\\
\frac{dI_L}{dt} &= \left(\lambda_1+\lambda_2\right) S_L + \alpha\, I_H - \left(\rho+\mu+\mu_d\right) I_L,\\
\frac{dI_H}{dt} &= \eta_2\left(\lambda_1+\lambda_2\right) S_H - \left(\alpha+\rho+\mu+\mu_d\right) I_H,\\
\frac{dR}{dt} &= \rho\left(I_L+I_H\right) - (\theta+\mu)\, R,\\
\frac{dB}{dt} &= \xi\left(I_L+\tau\, I_H\right) - d\, B,\\
\left(S_L(0),\, S_H(0),\, I_L(0),\, I_H(0),\, R(0),\, B(0)\right) &\in \mathbb{R}^6_+\cup\{0\}
\end{aligned}\right\} \tag{1}$$

The model parameters and their baseline values that will be used for numerical simulation later in the study are presented in Table 1.

For convenience, the following conventions are used whenever necessary:

$k_1 = \alpha+\mu$, $k_2 = \rho+\mu+\mu_d$, $k_3 = \alpha+\rho+\mu+\mu_d$, and $k_4 = \theta+\mu$. The following section delves into the fundamental qualitative characteristics of the model.

Qualitative properties of the cholera model

Positivity and boundedness of solutions of model

The following result proves that the model (1) is epidemiologically well-posed and also provides the region within which the model will be studied.

Lemma 1. *All solutions of the Cholera model (1) emanating from non-negative initial conditions are always non-negative. Also, system (1) admits a positively invariant region Ω given by*

$$\Omega = \left\{ \left(S_L(t),\, S_H(t),\, I_L(t),\, I_H(t),\, R(t),\, B(t)\right) \in \mathbb{R}^6_+ \,|\, N(t) \le \frac{\Lambda}{\mu} \;\text{ and }\; B(t) \le \frac{\xi\tau\Lambda}{d\mu} \right\}.$$

Proof. Define $\zeta(x) = \left\{x(t)=0 \text{ and } \left(S_L,\, S_H,\, I_L,\, I_H,\, R\right)\in\mathbb{R}^5_+,\, B\in\mathbb{R}_+\right\}$ and $x\in\left\{S_L,\, S_H,\, I_L,\, I_H,\, R,\, B\right\}$.

Then

$$\left\{\begin{aligned}
\left.\frac{dS_L}{dt}\right|_{\zeta(S_L)} &= (1-f)\,\Lambda + \alpha\, S_H + \theta\, R > 0,\\
\left.\frac{dS_H}{dt}\right|_{\zeta(S_H)} &= f\,\Lambda > 0,\\
\left.\frac{dI_L}{dt}\right|_{\zeta(I_L)} &= \left(\lambda_1+\lambda_2\right) S_L + \alpha\, I_H > 0,\\
\left.\frac{dI_H}{dt}\right|_{\zeta(I_H)} &= \eta_2\left(\lambda_1+\lambda_2\right) S_H > 0,\\
\left.\frac{dR}{dt}\right|_{\zeta(R)} &= \rho\left(I_L+I_H\right) > 0,\\
\left.\frac{dB}{dt}\right|_{\zeta(B)} &= \xi\left(I_L+\tau\, I_H\right) > 0.
\end{aligned}\right.$$

From [19, **Lemma 2**], it can be concluded that, any solution of model (1) is contained in $\mathbb{R}^6_+$.

Now, summing all equations involving human compartments in (1) gives

$$\frac{dN}{dt} = \Lambda - \mu\, N - \mu_d\left(I_L+I_H\right) \le \Lambda - \mu\, N,$$

so that upon solution, we have $\limsup_{t\to\infty} N(t) \le \frac{\Lambda}{\mu}$.

Further, from the last equation of model (1) we have

$$\frac{dB}{dt} = \xi\left(I_L+\tau\, I_H\right) - d\, B \le \xi\tau\, N - d\, B \le \frac{\xi\tau\Lambda}{\mu} - d\, B,$$

so that we have $\limsup_{t\to\infty} B(t) \le \frac{\xi\tau\Lambda}{d\mu}$. This concludes the proof. □

Fixed points and basic reproduction number of the cholera model (1)

In the absence of cholera, we have $I_L = I_H = R = B = 0$ and the cholera-free equilibrium is thus given by

$\mathcal{E}_0 = \left(S_{L0},\, S_{H0},\, 0,\, 0,\, 0,\, 0\right)$, where $S_{L0} = \frac{\Lambda(\alpha+\mu(1-f))}{\mu(\alpha+\mu)} = \frac{\Lambda(k_1-\mu f)}{k_1\mu}$ and $S_{H0} = \frac{f\Lambda}{\alpha+\mu} = \frac{f\Lambda}{k_1}$.

The basic reproduction number is a threshold parameter that describes the average number of non-primary infections that a primary infective will infect throughout its infectiousness cycle. There are a plethora of techniques that can be used to determine $\mathcal{R}_0$ for deterministic models like (1). Recently, a novel algebraic technique was developed for the computation of $\mathcal{R}_0$ [20]. This method is simpler than the famous Next-generation method [21]. In this study, we employed the Jacobian-Determinant method of [20] to determine $\mathcal{R}_0$. Using this method, the Jacobian of the infected subsystem of model (1) at $\mathcal{E}_0$ is given by;

$$\mathcal{J}_{\text{Inf}} = \begin{bmatrix}
\frac{\beta_h S_{L0}}{S_{L0}+S_{H0}} - k_2 & \frac{\beta_h\eta_1 S_{L0}}{S_{L0}+S_{H0}} + \alpha & \frac{\beta_b S_{L0}}{K}\\
\frac{\eta_2\beta_h S_{H0}}{S_{L0}+S_{H0}} & \frac{\eta_2\beta_h\eta_1 S_{H0}}{S_{L0}+S_{H0}} - k_3 & \frac{\eta_2\beta_b S_{H0}}{K}\\
\xi & \xi\tau & -d
\end{bmatrix}.$$

The determinant of $\mathcal{J}_{\text{Inf}}$ can be written as

$$\left|\mathcal{J}_{\text{Inf}}\right| = \left(\frac{\left(S_{H0}\left(\eta_1 k_2+\alpha\right)\eta_2 + S_{L0}k_3\right)\beta_h}{\left(S_{L0}+S_{H0}\right)k_2k_3} + \frac{\xi\left(\eta_2\left(\tau k_2+\alpha\right)S_{H0} + S_{L0}k_3\right)\beta_b}{Kdk_2k_3} - 1\right) dk_2k_3,$$

so that by the method in [20], $\mathcal{R}_0$ is obtained as

$$\mathcal{R}_0 = \frac{\beta_h\left(\eta_2\left(\eta_1 k_2+\alpha\right)S_{H0} + S_{L0}k_3\right)}{\left(S_{L0}+S_{H0}\right)k_2k_3} + \frac{\beta_b\left(S_{H0}\left(\tau\, k_2+\alpha\right)\eta_2 + S_{L0}k_3\right)\xi}{k_3k_2Kd},$$

or equivalently, upon substituting S_{L0} and S_{H0} we have $\mathcal{R}_0 = \mathcal{R}_{0h} + \mathcal{R}_{0b}$, where

$$\mathcal{R}_{0h} = \frac{\beta_h\left[\mu\left((1-f)k_3 + \eta_2 f\left(\eta_1 k_2+\alpha\right)\right) + \alpha\, k_3\right]}{k_1k_2k_3}$$

Table 2
Number of possible endemic fixed points of the cholera model (1).

Signs of Ψ_i for $\mathcal{R}_0 > 1$					Number of $\mathcal{E}^*$	Signs of Ψ_i for $\mathcal{R}_0 < 1$					Number of $\mathcal{E}^*$
Ψ_0	Ψ_1	Ψ_2	Ψ_3	Ψ_4		Ψ_0	Ψ_1	Ψ_2	Ψ_3	Ψ_4	
−	+	+	+	+	1	+	+	+	+	+	0
−	+	+	−	+	1, 3	+	+	+	−	+	0,2
−	+	−	+	+	1, 3	+	+	−	+	+	0,2
−	+	−	−	+	1,3	+	+	−	−	+	0,2
−	−	+	+	+	1	+	−	+	+	+	0,2
−	−	+	−	+	1,3	+	−	+	−	+	0,2,4
−	−	−	+	+	1	+	−	−	+	+	0,2
−	−	−	−	+	1	+	−	−	−	+	0,2

Table 3
Sensitivity of $\mathcal{R}_0$ and endemic equilibrium $\mathcal{E}^*$ to model parameters.

Par	Sensitivity index						
	$\mathcal{R}_0$	S_L^*	S_H^*	I_L^*	I_H^*	R^*	B^*
f	6.06×10^{-5}	−0.00211	1.0	-7.831×10^{-5}	1.0	6.57×10^{-5}	0.0001377
Λ	0.9997	0.002352	0.995	1.087	2.078	1.087	1.087
μ_d	−0.7872	0.7862	0.004884	−1.05	−1.099	−1.05	−1.05
τ	1.746×10^{-5}	−0.0002154	-1.09×10^{-6}	1.878×10^{-5}	0.0002327	1.882×10^{-5}	0.0002348
ρ	−0.2099	0.211	0.0001583	−0.03328	−0.04867	0.9667	−0.03328
θ	0.0000	−0.0002882	-6.677×10^{-5}	0.01403	0.01426	−0.9292	0.01403
d	−0.9997	0.9976	0.005048	−0.08699	−1.078	−0.08713	−1.087
β_b	0.9997	−1.001	−0.005066	0.08731	1.082	0.08745	0.08752
β_h	0.0002531	−0.002613	-1.322×10^{-5}	0.0002278	0.002822	0.0002282	0.0002284
K	−0.9997	0.9976	0.005048	−0.08699	−1.078	−0.08713	−0.0872
η_1	4.419×10^{-9}	-5.642×10^{-7}	-2.855×10^{-9}	4.919×10^{-8}	6.095×10^{-7}	4.927×10^{-8}	4.931×10^{-8}
η_2	0.0001702	−0.002103	−0.004663	4.088×10^{-5}	0.9956	0.0001842	0.0002559
ξ	0.9997	−0.9976	−0.005048	0.08699	1.078	0.08713	1.087
μ	−1.003	0.002436	0.0002705	−0.1053	−0.1048	−0.162	−0.1053
α	-6.6×10^{-5}	0.002167	−0.9951	0.0002059	−1.925	-7.122×10^{-5}	-2.097×10^{-4}

and $\mathcal{R}_{0b} = \dfrac{\Lambda \beta_b \xi \left[\mu\left((1-f)k_3 + \eta_2 f\left(\tau k_2 + \alpha\right)\right) + \alpha k_3\right]}{\mu k_1 k_2 k_3 K d}$.

The quantities $\mathcal{R}_{0h}$ and $\mathcal{R}_{0b}$ in $\mathcal{R}_0$ represent the basic reproduction numbers associated with infections from human contact(indirect transmission) and bacteria-infected environment (direct transmission) respectively. Therefore, from Lemma 2 of [21], we obtain Lemma 2.

Lemma 2. *Local asymptotic stability of the cholera-free fixed point $\mathcal{E}_0$ of (1) is guaranteed for $\mathcal{R}_0 < 1$. The stability is lost when $\mathcal{R}_0 > 1$.*

The epidemiological consequence of Lemma 2 is that it is possible to eradicate cholera from the population if the population is close enough to $\mathcal{E}_0$ and $\mathcal{R}_0$ can be kept below 1 for a sufficiently long period.

We turn our attention to the non-infected fixed point. To obtain the cholera-persistent equilibrium, let a typical endemic equilibrium be $\mathcal{E}^* = \left(S_L^*, S_H^*, I_L^*, I_H^*, R^*, B^*\right)$ and let $\lambda^* = \lambda_1^* + \lambda_2^*$, so that solving model (1) for non-trivial values of S_L^*, S_H^*, I_L^*, I_H^*, R^* and B^* gives;

$$\left.\begin{aligned}
S_L^* &= \tfrac{k_2 k_4 \Gamma_1}{k_2 k_4(\lambda^*+\mu)-\theta\rho\lambda^*},\\
S_H^* &= \tfrac{f\Lambda}{(\eta_2\lambda^*+k_1)},\\
I_L^* &= \tfrac{\lambda^*}{k_2}\left[\tfrac{k_2 k_4 \Gamma_1}{k_2 k_4(\lambda^*+\mu)-\theta\rho\lambda^*} + \tfrac{\alpha\eta_2 f\Lambda}{k_3(\eta_2\lambda^*+k_1)}\right],\\
I_H^* &= \tfrac{\eta_2 f\Lambda\lambda^*}{k_3(\eta_2\lambda^*+k_1)},\\
R^* &= \tfrac{\rho}{k_4}\left(I_L^* + I_H^*\right),\\
B^* &= \tfrac{\xi}{d}\left(I_L^* + \tau I_H^*\right),\\
\Gamma_1 &= (1-f)\Lambda + \tfrac{f\Lambda}{(\eta_2\lambda^*+k_1)}\left(\alpha + \tfrac{\theta\rho\eta_2\lambda^*}{k_2 k_4}\right).
\end{aligned}\right\} \quad (2)$$

Now, substituting appropriate equilibrium values into $\lambda = \lambda_1 + \lambda_2$ gives,

$$\lambda^* = \frac{\beta_h\left(I_L^* + \eta_1 I_H^*\right)}{N^*} + \frac{\beta_b B^*}{K + B^*},$$

and simplifying, yields the following polynomial equation.

$$\lambda^*\left[\Psi_4\left(\lambda^*\right)^4 + \Psi_3\left(\lambda^*\right)^3 + \Psi_2\left(\lambda^*\right)^2 + \Psi_1\lambda^* + \Psi_0\right] = 0, \quad (3)$$

where

$$\begin{aligned}
\Psi_4 &= \Lambda\eta_2^2\left(k_4\mu_d + x_3\right)\left[\Lambda\xi\left(A_1 - k_4\right) + dKx_3\right],\\
\Psi_3 &= \left[\Lambda\eta_2\left(k_4 - A_1\right)\xi - dK\eta_2 x_3\right]\left[\Lambda\left(\eta_2\mu k_2 k_4 - k_1 x_3\right)\right.\\
&\quad \left. + \mu\Lambda\eta_2\left(A_2 - k_4\right)\beta_h - A_4\mu_d\right]\\
&\quad -\Lambda\eta_2\left(k_4\mu_d + x_3\right)\left[dK\left(\eta_2\mu k_2 k_4 - k_1 x_3\right)\right.\\
&\quad \left. +\xi\left(\Lambda\eta_2\left(A_1 - k_4\right)\beta_h + A_5\right)\right],\\
\Psi_2 &= -\Lambda dKk_1\mu k_2 k_4\eta_2 x_3\left(2 - \mathcal{R}_0\right) - \Lambda\eta_2 k_4\mu_d\left(k_1\mu k_2 k_4 dK - A_4\xi\beta_b\right)\\
&\quad -\Lambda^2 k_1\mu k_2 k_4\eta_2\left(A_1 - k_4\right)\xi\\
&\quad +\Lambda\left(\eta_2\mu k_2 k_4 - \eta_2\left(A_2 - k_4\right)\mu_d - k_1 x_3\right)\left[dK\left(\eta_2\mu k_2 k_4 - k_1 x_3\right)\right.\\
&\quad \left. +\xi\left(\Lambda A_1\beta_h\eta_2 - \Lambda\beta_h\eta_2 k_4 + A_4\right)\right]\\
&\quad +\left[\left(\mu\left(A_1 - k_4\right)A_5 + \mu\left(A_2 - k_4\right)A_4\right)\xi + \mu\left(A_2 - k_4\right)dK\right.\\
&\quad \left.\times\left(\eta_2\mu k_2 k_4 - k_1 x_3\right)\right]\eta_2\Lambda\beta_h,\\
\Psi_1 &= \Lambda dKk_1\mu k_2 k_4\left(\eta_2\mu k_2 k_4 - k_1 x_3\right)\left(2 - \mathcal{R}_0\right)\\
&\quad +\mu\beta_h\left(dK\mu\Lambda\eta_2 A_2 k_1 k_2 k_4 - \xi A_5 A_6\right)\\
&\quad +\xi\left(\Lambda^2 k_1\mu\eta_2 k_2 k_4 A_1 + A_4 A_5\mu_d\right)\beta_b + \mu k_1 k_2 k_4\\
&\quad \times\left(\Lambda\xi A_5 - K\mu_d dA_4\right),\\
\Psi_0 &= \Lambda {k_1}^2\mu^2 {k_2}^2 {k_4}^2 dK\left(1 - \mathcal{R}_0\right),\\
A_1 &= \tfrac{f(\tau-1)x_3}{k_3}, \quad A_2 = \tfrac{f(\eta_1-1)x_3}{k_3}, \quad A_3 = k_4\Lambda\left(\mu f\left(\eta_2 - 1\right) + k_1\right),\\
A_4 &= \tfrac{f\Lambda\eta_2(\tau k_2+\alpha)\mu k_4}{k_3} + \tfrac{\Lambda x_2}{k_2 k_3}, \quad A_5 = \tfrac{f\Lambda\eta_2(\eta_1 k_2+\alpha)\mu k_4}{k_3} + \tfrac{\Lambda x_2}{k_2 k_3},\\
x_1 &= \eta_2 k_3\left[f\rho\theta + k_2 k_4(1-f)\right],\ x_2 = k_2 k_3 k_4\left[k_1(1-f) + \alpha f\right],\\
x_3 &= \rho\theta - k_2 k_4.
\end{aligned}$$

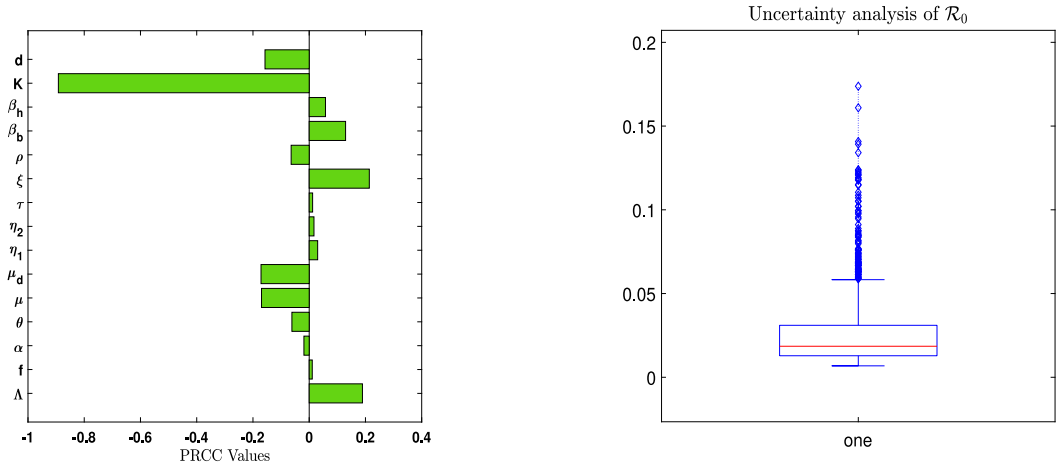

(a) PRCC plot for cholera in the presence of hyper-infective individuals.

(b) The box plot of $\mathcal{R}_0$.

Fig. 1. Global sensitivity and uncertainty analysis of $\mathcal{R}_0$.

The solution $\lambda^* = 0$ of Eq. (3) corresponds to the cholera-free equilibrium while the cholera-persistent equilibrium is characterized by the quartic part of Eq. (3).

It is easy to establish that $\Psi_4 > 0$ and clearly $\Psi_0 < 0$ whenever $\mathcal{R}_0 > 1$. The number of positive cholera-persistent equilibria of the model (1) then will depend on the coefficients Ψ_1, Ψ_2 and Ψ_3 and are given in Table 2.

Sensitivity analysis

Model behaviour and predictions are determined by model parameters whose measurements are bedevilled with uncertainties due to the unavailability of required data or measurement errors. For this reason, the reliability of model predictions needs to be considered well during the modelling process. Sensitivity analysis aims to explore the influence of small perturbations in model parameters (inputs) on the predictions generated by the model (output) [22,23]. This process assists in identifying parameters with significant sensitivity values, which should be prioritized for accurate data collection. Additionally, sensitivity indices provide insight into which parameters can be focused on and adjusted to attain the intended outcomes.

To determine the sensitivity indexes of $\mathcal{R}_0$ to model parameters, we employ the normalized forward sensitivity index defined by $\Upsilon^p_{\mathcal{R}_0} = \frac{\partial \mathcal{R}_0}{\partial p} \times \frac{p}{\mathcal{R}_0}$, where p is a parameter upon which $\mathcal{R}_0$ depends differentiably. Since the persistence of cholera is associated with the cholera-persistent fixed point, we also conducted a sensitivity analysis of the cholera-persistent fixed point with the aid of the technique developed in [24]. The functional forms of the sensitivity indexes of most of the parameters are complex, and hence we present their numerical values in Table 3 using the values of parameters given in Table 1.

It can be observed from Table 3 that the predominant factors influencing $\mathcal{R}_0$ and consequently disease progression include the human natural death rate μ, closely followed by the human inflow rate Λ, the rate at which *Vibrio cholerae* is removed from the environment d, the pathogen ingestion rate from the contaminated environment β_b, the environment's capacity to sustain the pathogen K, the pathogen shedding rate into the environment by infected individuals ξ, and the death rate in humans due to cholera μ_d. These are the parameters with the highest sensitivity indexes when dealing with $\mathcal{R}_0$. Attempts to control cholera spread should be targeted at reducing $\mathcal{R}_0$, which can be done by reducing those parameters (Λ, β_b, and ξ) with positive indices while increasing those parameters (μ, d, K, and μ_d) with negative indices. Doing this will ultimately reduce the number of infectives and control the spread of cholera.

Optimal control of cholera

Attempts to control the spread of cholera involve avoiding or reducing infection, increasing adherence to healthy sanitation protocols, reducing bacterial shedding, and treating water supply systems. This section incorporates these controls into the basic model (1) to produce an optimal control problem. The control problem involves minimizing a certain metric subject to the modified model. With this, the goal is to determine the most cost-effective strategies that can be adopted to fight the spread of cholera. We define the following controls:

(1) Control for preventing/reducing contact with infection sources, $u_1(t)$;
(2) Control for increasing adherence to healthy protocols of sanitation, $u_2(t)$;
(3) Control for treatment of the infected persons, $u_3(t)$ and
(4) Control for reducing bacterial-shedding, $u_4(t)$.

With these controls, the following optimal control problem is in order.

$$\left.\begin{aligned}
&\min \mathcal{J}(u) = \int_0^T \left(m_1 S_H + m_2 I_L + m_3 I_H + m_4 B + \sum_{i=1}^{4} \omega_i u_i^2 \right) \mathrm{d}t, \\
&\text{Subject to:} \\
&\frac{\mathrm{d}S_L}{\mathrm{d}t} = (1-f)\Lambda + \alpha u_2 S_H + \theta R - \left((1-u_1)(\lambda_1+\lambda_2) + \mu\right) S_L, \\
&\frac{\mathrm{d}S_H}{\mathrm{d}t} = f\Lambda - \left(\eta_2(\lambda_1+\lambda_2)(1-u_1) + \alpha u_2 + \mu\right) S_H, \\
&\frac{\mathrm{d}I_L}{\mathrm{d}t} = (\lambda_1+\lambda_2)(1-u_1) S_L + \alpha u_2 I_H - \left(\rho u_3 + \mu + \mu_d\right) I_L, \\
&\frac{\mathrm{d}I_H}{\mathrm{d}t} = \eta_2(\lambda_1+\lambda_2)(1-u_1) S_H - \left(\alpha u_2 + \rho u_3 + \mu + \mu_d\right) I_H, \\
&\frac{\mathrm{d}R}{\mathrm{d}t} = \rho u_3 (I_L + I_H) - (\theta + \mu) R, \\
&\frac{\mathrm{d}B}{\mathrm{d}t} = \xi (1-u_4)(I_L + \tau I_H) - dB.
\end{aligned}\right\} \quad (4)$$

The coefficients, m_i, $i = 1, 2 \ldots, 4$ are positive weights associated with the state variable, ω_i, $i = 1, 2 \ldots, 4$ are unit costs of implementing the associated controls.

The main goal is to minimize the cost and to reduce hyper-susceptibility, infected persons and *Vibrio cholerae* concentration. Thus, an optimal quadruple $u^* = \left(u_1^*, u_1^*, u_2^*, u_3^*, u_4^*\right)$ that minimizes the functional $\mathcal{J}$ over the set of admissible control, $\mathcal{U}$ is being sought. Thus, the goal is to find u^* such that $\mathcal{J}(u^*)$ is the minimum of $\mathcal{J}(u)$ over the set of admissible controls defined as $\mathcal{U} = \left\{u_i : u_i \text{ is measurable with } 0 \le u_i \le 1, i = 1, 2 \ldots, 4\right\}$.

The conditions precedent for the pair $(u^*,\ x^*)$ to be optimal are provided by the Pontryagin's principle [25], where $x^* = (S_L^*,\ S_H^*,\ I_L^*,\ I_H^*,\ R^*,\ B^*)$. This principle transforms the optimal control problem into a problem of point-wise minimization of a Hamiltonian given by

$$\mathcal{H} = \frac{\mathrm{d}\mathcal{J}}{\mathrm{d}t} + \lambda_{S_L}\frac{\mathrm{d}S_L}{\mathrm{d}t} + \lambda_{S_H}\frac{\mathrm{d}S_H}{\mathrm{d}t} + \lambda_{I_L}\frac{\mathrm{d}I_L}{\mathrm{d}t} + \lambda_{I_H}\frac{\mathrm{d}I_H}{\mathrm{d}t} + \lambda_R\frac{\mathrm{d}R}{\mathrm{d}t} + \lambda_B\frac{\mathrm{d}B}{\mathrm{d}t},$$

where λ_{S_L}, λ_{S_H}, λ_{I_L}, λ_{I_H}, λ_R and λ_B are adjoint variables corresponding to the state variables S_L, S_H, I_L, I_H, R and B respectively.

Based on the Pontryagin's Principle [25,26], the following theorem is established.

Theorem 3. *If the quadruple $(u_1^*, u_2^*, u_3^*, u_4^*)$ minimizes the functional $\mathcal{J}$ over $\mathcal{U}$, then there exist adjoint variables λ_{S_L}, λ_{S_H}, λ_{I_L}, λ_{I_H}, λ_R and λ_B associated with S_L, S_H, I_L, I_H, R and B respectively such that the following hold:*

(i) $\frac{\mathrm{d}\lambda_{S_L}}{\mathrm{d}t} = -\frac{\mathrm{d}\mathcal{H}}{\mathrm{d}S_L}$, $\frac{\mathrm{d}\lambda_{S_H}}{\mathrm{d}t} = -\frac{\mathrm{d}\mathcal{H}}{\mathrm{d}S_H}$, $\frac{\mathrm{d}\lambda_{I_L}}{\mathrm{d}t} = -\frac{\mathrm{d}\mathcal{H}}{\mathrm{d}I_L}$, $\frac{\mathrm{d}\lambda_{I_H}}{\mathrm{d}t} = -\frac{\mathrm{d}\mathcal{H}}{\mathrm{d}I_H}$, $\frac{\mathrm{d}\lambda_R}{\mathrm{d}t} = -\frac{\mathrm{d}\mathcal{H}}{\mathrm{d}R}$, *and* $\frac{\mathrm{d}\lambda_B}{\mathrm{d}t} = -\frac{\mathrm{d}\mathcal{H}}{\mathrm{d}B}$.

(ii) $\lambda_{S_L}(T) = \lambda_{S_H}(T) = \lambda_{I_L}(T) = \lambda_{I_H}(T) = \lambda_R = \lambda_B(T) = 0$: *Transversality conditions.*

(iii) $u_i^* = \min\left\{1,\ \max\left\{0,\ \widetilde{u_i}\right\}\right\}$, *Stationary values, where*

$$\widetilde{u_1} = \frac{(\lambda_1+\lambda_2)}{2\omega_1}\left[\eta_2 S_H\left(\lambda_{I_H}-\lambda_{S_H}\right) + S_L\left(\lambda_{I_L}-\lambda_{S_L}\right)\right],$$
$$\widetilde{u_2} = \frac{\alpha}{2\omega_2}\left[\left(\lambda_{I_L}-\lambda_{I_H}\right) I_H + S_H\left(\lambda_{S_L}-\lambda_{S_H}\right)\right],$$
$$\widetilde{u_3} = \frac{\rho}{2\omega_3}\left[\left(\lambda_R-\lambda_{I_L}\right) I_L + \left(\lambda_R-\lambda_{I_H}\right) I_H\right],$$
$$\widetilde{u_4} = \frac{\lambda_B\xi\left(\tau I_H + I_L\right)}{2\omega_4}.$$

Therefore, the problem of solving the optimal control problem becomes a problem of solving the following system of ordinary differential equations:

$$\left.\begin{aligned}
\frac{\mathrm{d}S_L}{\mathrm{d}t} &= (1-f)\Lambda + \alpha u_2^* S_H + \theta R - \left(\left(1-u_1^*\right)\left(\lambda_1+\lambda_2\right)+\mu\right) S_L,\\
\frac{\mathrm{d}S_H}{\mathrm{d}t} &= f\Lambda - \left(\eta_2\left(\lambda_1+\lambda_2\right)\left(1-u_1^*\right)+\alpha u_2^*+\mu\right) S_H,\\
\frac{\mathrm{d}I_L}{\mathrm{d}t} &= \left(\lambda_1+\lambda_2\right)\left(1-u_1^*\right) S_L + \alpha u_2^* I_H - \left(\rho u_3^*+\mu+\mu_d\right) I_L,\\
\frac{\mathrm{d}I_H}{\mathrm{d}t} &= \eta_2\left(\lambda_1+\lambda_2\right)\left(1-u_1^*\right) S_H - \left(\alpha u_2^*+\rho u_3^*+\mu+\mu_d\right) I_H,\\
\frac{\mathrm{d}R}{\mathrm{d}t} &= \rho u_3^*\left(I_L+I_H\right) - (\theta+\mu) R,\\
\frac{\mathrm{d}B}{\mathrm{d}t} &= \xi\left(1-u_4^*\right)\left(I_L+\tau I_H\right) - dB,\\
\frac{\mathrm{d}\lambda_{S_L}}{\mathrm{d}t} &= \left[\eta_2\frac{\lambda_1 S_H}{N}\left(\lambda_{I_H}-\lambda_{S_H}\right) + \left(\lambda_{I_L}-\lambda_{S_L}\right)\left(\frac{\lambda_1 S_L}{N}-\lambda_1-\lambda_2\right)\right]\\
&\quad\times\left(1-u_1^*\right) + \lambda_{S_L}\mu,\\
\frac{\mathrm{d}\lambda_{S_H}}{\mathrm{d}t} &= \left[\frac{\lambda_1 S_L}{N}\left(\lambda_{I_L}-\lambda_{S_L}\right) + \eta_2\left(\lambda_{I_H}-\lambda_{S_H}\right)\left(\frac{\lambda_1 S_H}{N}-\lambda_1-\lambda_2\right)\right]\\
&\quad\times\left(1-u_1^*\right)\\
&\quad+\lambda_{S_H}\mu - m_1 + \left(\lambda_{S_H}-\lambda_{S_L}\right)\alpha u_2^*,\\
\frac{\mathrm{d}\lambda_{I_L}}{\mathrm{d}t} &= \left(\frac{\beta_h}{N}-\frac{\lambda_1}{N}\right)\left[\eta_2 S_H\left(\lambda_{S_H}-\lambda_{I_H}\right) + S_L\left(\lambda_{S_L}-\lambda_{I_L}\right)\right]\left(1-u_1^*\right)\\
&\quad+\lambda_{I_L}\left(\mu+\mu_d\right) - m_2 + \left(\lambda_{I_L}-\lambda_R\right)\rho u_3^* - \lambda_B\xi\left(1-u_4^*\right),\\
\frac{\mathrm{d}\lambda_{I_H}}{\mathrm{d}t} &= \left(\frac{\beta_h\eta_1}{N}-\frac{\lambda_1}{N}\right)\left[\eta_2 S_H\left(\lambda_{S_H}-\lambda_{I_H}\right) + S_L\left(\lambda_{S_L}-\lambda_{I_L}\right)\right]\\
&\quad\times\left(1-u_1^*\right) - m_3\\
&\quad+\lambda_{I_H}\left(\mu+\mu_d\right) + \left(\lambda_{I_H}-\lambda_{I_L}\right)\alpha u_2^* + \left(\lambda_{I_H}-\lambda_R\right)\rho u_3^*\\
&\quad-\lambda_B\xi\left(1-u_4^*\right)\tau,\\
\frac{\mathrm{d}\lambda_R}{\mathrm{d}t} &= \lambda_R\mu + \frac{\lambda_1}{N}\left[\eta_2 S_H\left(\lambda_{I_H}-\lambda_{S_H}\right) + S_L\left(\lambda_{I_L}-\lambda_{S_L}\right)\right]\left(1-u_1^*\right)\\
&\quad+\theta\left(\lambda_R-\lambda_{S_L}\right),\\
\frac{\mathrm{d}\lambda_B}{\mathrm{d}t} &= \lambda_B d + \frac{K\beta_b}{(K+B)^2}\left[\eta_2 S_H\left(\lambda_{S_H}-\lambda_{I_H}\right) + S_L\left(\lambda_{S_L}-\lambda_{I_L}\right)\right]\\
&\quad\times\left(1-u_1^*\right) - m_4,\\
\lambda_{S_L}(T) &= \lambda_{S_H}(T) = \lambda_{I_L}(T) = \lambda_{I_H}(T) = \lambda_R = \lambda_B(T) = 0.
\end{aligned}\right\} \quad (5)$$

Table 4
List of all control combinations.

Strategy	Control combination	Strategy	Control combination
0	None	8	Only u_2 and u_3
1	Only u_1	9	Only u_2 and u_4
2	Only u_2	10	Only u_3 and u_4
3	Only u_3	11	Only u_1, u_2 and u_3
4	Only u_4	12	Only u_1, u_2 and u_4
5	Only u_1 and u_2	13	Only u_1, u_3 and u_4
6	Only u_1 and u_3	14	Only u_2, u_3 and u_4
7	Only u_1 and u_4	15	All controls

Numerical simulation

In this section, numerical experiments are conducted firstly to illustrate the global sensitivity analysis using the partial rank coefficient correlation plot, followed by the analytical results discussed earlier and to present further model analysis. The baseline parameter values in Table 1 are used throughout the simulation unless otherwise stated.

The global sensitivity indexes of the parameters in $\mathcal{R}_0$ are depicted in Fig. 1(a) and follow the same trend as the local sensitivity analysis. Fig. 1(a) shows that ξ, the rate at which infected people shed bacteria, is the most sensitive parameter in the basic reproduction number, followed by Λ, the rate at which humans are recruited, β_b, the rate at which the bacteria are ingested from the environment, and finally β_h, the rate at which humans ingest them. Similarly, we observe that the concentration of Vibrio cholerae (represented by K), the rate at which the bacteria are eliminated (represented by μ), the rate at which humans die from cholera (represented by μ_d), and the rate at which humans die naturally (represented by μ) are all negatively correlated with the basic reproduction number. Fig. 1(b) from the uncertainty analysis shows that the $\mathcal{R}_0$ ranges from about $[0-0.2]$, with most outputs clustered near the lower end of that range ($[0-0.05]$).

To illustrate the local stability of equilibria (See Fig. 2), the model (1) is ran (for both when of $\mathcal{R}_0 < 1$ and when $\mathcal{R}_0 > 1$) with different initial conditions.

Fig. 2 illustrates that the cholera-free equilibrium $\mathcal{E}_0$ and cholera-persistent equilibrium $\mathcal{E}^*$ are locally asymptotically stable whenever $\mathcal{R}_0 < 1$ and $\mathcal{R}_0 > 1$ respectively.

The force of infection λ^* at equilibrium is also plotted against $\mathcal{R}_0$ in the bifurcation diagram in Fig. 3.

Fig. 3 indicates that the model exhibits forward bifurcation, which implies that the cholera-free equilibrium cannot coexist with a cholera-persistent equilibrium and that the condition $\mathcal{R}_0 < 1$ is sufficient for cholera eradication. Thus, if $\mathcal{R}_0$ can be kept below unity, then cholera can be eradicated when dealing with the proposed model.

Next, the State and co-state system (5) was converted into a boundary value problem, which was solved using the MATLAB *bvp4c* function. Due to the scarcity of resources, it may not be economical to consider a 100% implementation of all controls, and hence, it is important to determine which combination of the controls is most cost-effective at combatting the spread of cholera. The optimal control problem (4) is solved for all possible combinations of the controls while determining the high-risk susceptibles averted and the total infections averted, representing the difference between total outputs without control and the same with controls. Table 4 presents all the possible combinations of the controls for the optima control problem.

Results of the numerical simulations are presented in Table 5, where the S_H, I_L, and I_H columns, respectively, represent the number of high-risk susceptibles, low-risk Infectives, and High-risk infectives averted when the associated strategies are implemented. The $X = S_H + I_L + I_H$ column is the sum of undesirable groups averted for the strategies. The J column presents the value of the objective functional for the strategy.

The Incremental Cost-Effectiveness Ratio (ICER) is utilized to ascertain the most economically efficient approaches. The ICER serves as a

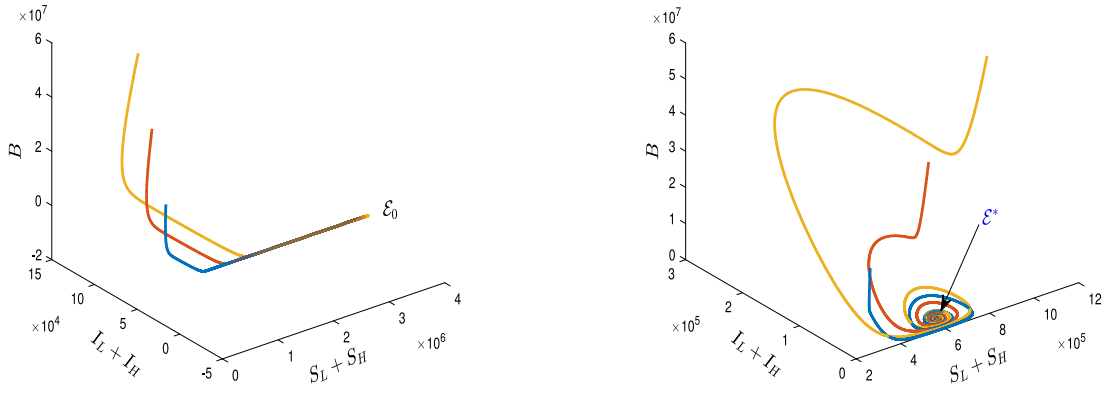

(a) For $\mathcal{R}_0 < 1$ (b) For $\mathcal{R}_0 > 1$

Fig. 2. Plots of susceptibles, infective and bacteria showing dependence of local stability of equilibria on $\mathcal{R}_0$.

Table 5
Results from simulation of optimal control problem.

Strategy	Total averted				J	Cost (ℂ)
	S_H	I_1	I_2	$S_H + I_L + I_H$		
1	−1 262 049	7 215 727	6 344 219	12 297 896.73	1.7911×10^{10}	162.3573
2	−660 763	-8.2×10^7	−3 756 883	−86 278 884.41	7.7554×10^{11}	5047.913
3	209 447.8	5 013 388	4 412 371	9 635 206.842	3.1886×10^{10}	310
4	209 416.5	4 964 553	4 376 391	9 550 361.451	3.2877×10^{10}	320
5	−1 176 390	1 771 238	6 304 978	6 899 825.958	5.3423×10^{11}	10 455.78
6	−1 442 073	7 208 728	6 338 094	12 104 749.32	1.9897×10^{10}	302.9345
7	−812 016	7 245 165	6 369 973	12 803 122.56	1.2925×10^{10}	223.0752
8	−660 718	-8.2×10^7	−3 755 748	−86 063 970.45	7.7355×10^{11}	12 787.77
9	194 803.7	1 722 962	6 343 732	8 261 498.433	4.2854×10^{10}	656.7725
10	209 354.1	4 853 201	4 288 968	9 351 522.906	3.4863×10^{10}	635.6355
11	220 191.8	6 832 157	6 407 113	13 459 461.54	4.9789×10^{10}	1306.648
12	54 889.12	−841 462	6 725 268	5 938 695.063	8.0086×10^{11}	21 798.65
13	−992 040	7 238 171	6 363 853	12 609 984.12	1.4911×10^{10}	323.6527
14	194 778	1 708 105	6 343 710	8 246 593.849	4.384×10^{10}	1043.055
15	205 427.2	6 744 773	6 406 008	13 356 208.52	5.9743×10^{10}	2176.156

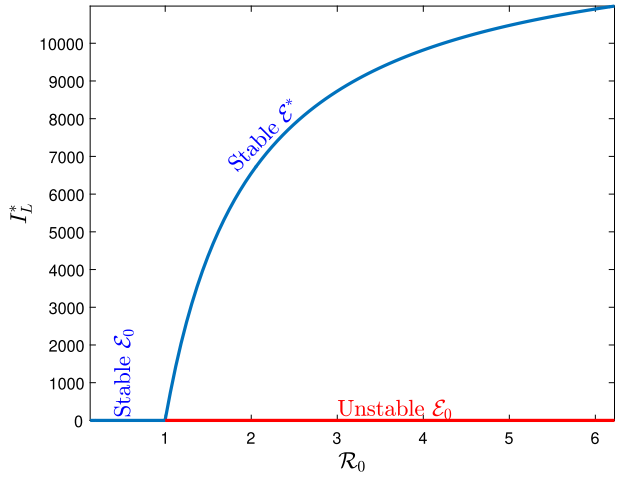

Fig. 3. Bifurcation diagram.

tool for contrasting the cost and benefits of alternative strategies, and its definition is as follows:

In the case where strategies X and Y yield benefits of X_b and Y_b respectively, along with corresponding costs of X_c and Y_c respectively, the calculation of the cost-effectiveness ratio for strategies X and Y is given by:

$$\text{ICER}(X) = \frac{X_b}{X_c}, \quad \text{ICER}(Y) = \frac{Y_b - X_b}{Y_c - X_c},$$

In this context, the reference strategy denoted as X represents the strategy with minimal benefit. The strategy having the lowest ICER value is considered the most economically efficient choice. Using this methodology, the strategies were ranked using the different outputs in Table 6, where each column represents the ranking of the strategies from best to least cost-effective if the corresponding heading is taken as the target. For example, if the target is to minimize the high-risk susceptibles and Infectives, $S_H + I_L + I_H$, the best strategy is to implement strategy 11, which involves only controls u_1, u_2 and u_3.

Fig. 4 presents the plot of infective populations for the overall best strategy (strategy 2) and that of the baseline strategy. Implementing the strategy leads to an increase in low-risk infectives and a reduction in the high-risk infectives. This will ultimately lead to a reduction in the spread of the disease. Also, Fig. 5 presents the control u_2 profile for the overall best strategy. It is observed that to achieve the goal of minimizing the functional, the control should be started at 100% implementation up to about the 5th day, then taken off up to the 78th day, followed by a 100% implementation up to the 85th day, and then gradually reduced to about 60% implementation and maintained at that level up to the 115th day, then a gradual increase until it reaches 100% on the 120th day. This is maintained until the implementation period ends when the control is taken off.

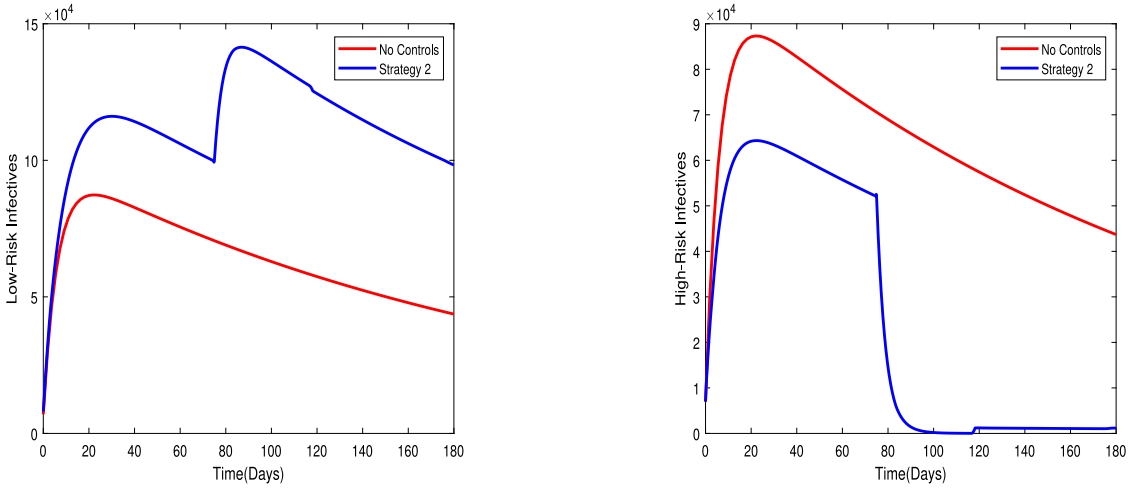

Fig. 4. Graphical comparison of strategy 2 and the baseline strategy.

Table 6
Ranking of strategies for various outputs ($X = S_H + I_L + I_H$).

S_H	3	4	10	11	9	14	15	12	7	13	2	1	6	5	8
I_L	7	1	6	13	11	3	4	10	15	9	14	5	2	8	12
I_H	11	7	1	13	9	6	14	15	3	4	10	5	12	2	8
X	11	7	1	6	13	3	4	10	9	14	15	5	12	2	8
J	2	8	5	12	9	3	4	1	6	10	7	13	14	11	15

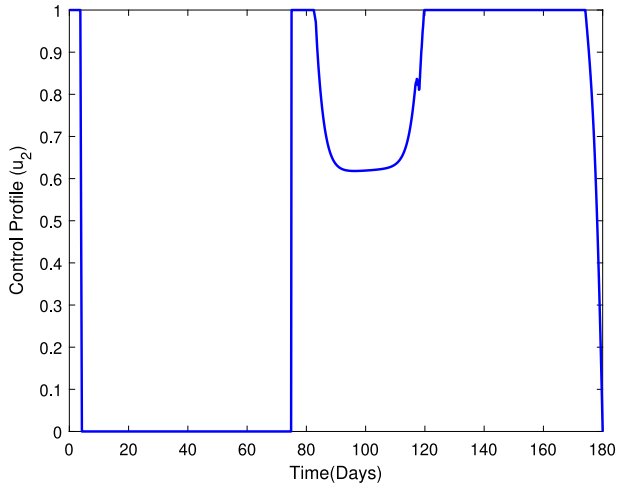

Fig. 5. Profile of control u_2 for the overall best strategy.

Conclusion

In this paper, a deterministic ordinary differential equation model is formulated to depict the dynamics of cholera in a population, considering human-to-human and environment-to-human transmission routes. The impact of varying behavioural levels among Susceptibles and Infectives regarding adopting effective sanitation protocols for preventing the spread of Cholera was also considered. The susceptible and infective populations were each divided into two sub-groups: those with proper etiquette towards controlling the spread of the disease and those without such good etiquette. The impact of varying behavioural levels among Susceptibles and Infectives regarding adopting effective sanitation protocols for preventing the spread of Cholera was also considered. To compare the effectiveness of various control strategies, we extended the basic model into an optimal control problem, intending to minimize infections and high-risk Susceptible persons and the associated cost. By employing Pontryagin's maxim principle [25], the optimal control problem is converted into a coupled system of state and co-state equations, which are numerically solved with MATLAB. Using Incremental Cost-Effectiveness Ratio (ICER) analysis, we compared the various combinations of interventions and showed that observance of good sanitation practices is the most cost-effective strategy for controlling the spread of cholera. Numerical simulation of the optimal control problem showed that promoting adherence to sanitation protocols is the most cost-effective strategy for fighting the spread of cholera. This finding is in line with that of Mwasa and Tchuenche [27], which suggested that improving the safety of drinking water and adequate sanitation are the best strategies in preventing the spread of cholera. While this study presents interesting results concerning the dynamics and control of cholera, we note that other very important factors such as seasonality of incidence rate; time delay; and quarantine of infected persons, could be incorporated into the model. These important aspects of the modelling are subjects of future study.

CRediT authorship contribution statement

Baba Seidu: Conceptualization, Methodology, Formal analysis, Writing – original draft, Writing – review & editing. **Eric N. Wiah:** Conceptualization, Methodology, Formal analysis, Writing – original draft, Writing – review & editing. **Joshua Kiddy K. Asamoah:** Conceptualization, Methodology, Formal analysis, Writing – original draft, Writing – review & editing.

Declaration of competing interest

The authors declare that they have no known competing financial interests or personal relationships that could have appeared to influence the work reported in this paper.

Data availability

No data was used for the research described in the article.

References

[1] Ali M, Nelson AR, Lopez AL, Sack DA. Updated global burden of cholera in endemic countries. PLoS Negl Trop Dis 2015.

[2] World Health Orgainzation. Cholera vaccines: Who position paper. 2017.

[3] Capasso V, Paveri-Fontana SL. A mathematical model for the 1973 cholera epidemic in the european mediterranean region. Rev dpidmol sant Publ 1979;27(121).

[4] Codeço Cláudia Torres. Endemic and epidemic dynamics of cholera: the role of the aquatic reservoir. BMC Infect Dis 2001;1:1.

[5] Neilan Rachael L Miller, Schaefer Elsa, Gaff Holly, Renee Fister K, Lenhart Suzanne. Modeling optimal intervention strategies for cholera. Bull Math Biol 2010;72:2004–18.

[6] Andrews Jason R, Basu Sanjay. Transmission dynamics and control of cholera in haiti: an epidemic model. Lancet 2011;377.

[7] Zhou Xueyong, Cui Jingan. Modeling and stability analysis for a cholera model with vaccination. Math Methods Appl Sci 2011;34.

[8] Wang Shu, Jin Liao. A generalized cholera model and epidemic-endemic analysis. J Biol Dyn 2012;6.

[9] Gupta Rabindra Kumar, Pal Soumitra, Misra AK. Modeling the impact of precautionary measures and sanitation practices broadcasted through media on the dynamics of bacterial diseases. Model Earth Syst Environ 2022;1–16.

[10] Misra AK, Gupta Alok, Venturino Ezio. Cholera dynamics with bacteriophage infection: a mathematical study. Chaos Solitons Fractals 2016;91:610–21.

[11] Lata Kusum, Misra AK, Takeuchi Y. Modeling the effectiveness of tv and social media advertisements on the dynamics of water-borne diseases. Int J Biomath 2022;15(02):2150069.

[12] Okosun OD, Makinde KO. A co-infection model of malaria and cholera diseases with optimal control. Math Biosci 2014;258:19–32.

[13] Zhou Jing-an, Xue-yong Cui. Threshold dynamics for a cholera epidemic model with periodic transmission rate. Appl Math Model 2013;37:3093–101.

[14] Seidu Baba, Bornaa CS, Makinde Oluwole D. An ebola model with hyper-susceptibility. Chaos Solitons Fractals 2020;138:109938.

[15] Seidu B, Makinde O, Bornaa CS. Mathematical analysis of an industrial HIV/AIDS model that incorporates carefree attitude towards sex. Acta Biotheor 2021;69(3):257–76.

[16] Levine MM, Black RE, Clements ML, Cisneros L, Nalin DR, Young CR. Duration of infection-derived immunity to cholera. J Infect Dis 1981;143:818–20.

[17] Mukandavire Z, Garira W. Sex-structured HIV/AIDS model to analyse the effects of condom use with application to zimbabwe. J Math Biol 2007;54(5):669–99.

[18] Hartley David M, Morris J Glenn, Smith David L. Hyperinfectivity: a critical element in the ability of v, cholerae to cause epidemics?. PLoS Med 2006;3:e7.

[19] Yang Xia, Chen Lansun, Chen Jufang. Permanence and positive periodic solution for the single-species nonautonomous delay diffusive models. Comput Math Appl 1996;32:109–16.

[20] Seidu B, Makinde OD, Asamoah JKK. Threshold quantities and lyapunov functions for ordinary differential equations epidemic models with mass action and standard incidence functions. Chaos Solitons Fractals 2023;170:113403.

[21] Shuai P, Zhisheng, van den Driessche. Global stability of infectious disease models using lyapunov functions. SIAM J Appl Math 2013;73.

[22] Asamoah Joshua Kiddy K, Jin Zhen, Sun Gui-Quan, Seidu Baba, Yankson Ernest, Abidemi Afeez, Oduro FT, Moore Stephen E, Okyere Eric. Eric sensitivity assessment and optimal economic evaluation of a new COVID-19 compartmental epidemic model with control interventions. Chaos Solitons Fractals 2021;146:110885.

[23] Asamoah Joshua Kiddy K, Jin Zhen, Sun Gui-Quan, Li Michael Y, et al. A deterministic model for Q fever transmission dynamics within dairy cattle herds: using sensitivity analysis and optimal controls. Comput Math Methods Med 2020. 2020.

[24] Chitnis Nakul, Hyman James M, Cushing Jim M. Determining important parameters in the spread of malaria through the sensitivity analysis of a mathematical model. Bull Math Biol 2008;70:1272–96.

[25] Pontryagin Lev Semenovich. The mathematical theory of optimal processes, Vol. 4. CRC Press; 1962.

[26] Asamoah Joshua Kiddy K, Okyere Eric, Abidemi Afeez, Moore Stephen E, Sun Gui-Quan, Jin Zhen, Acheampong Edward, Gordon Joseph Frank. Optimal control and comprehensive cost-effectiveness analysis for COVID-19. Results Phys 2022;33:105177.

[27] Mwasa A, Tchuenche JM. Mathematical analysis of a cholera model with public health interventions. Biosystems 2011;105.